Asian Journal of Chemistry; Vol. 38, No. 3 (2026), 651-658
ASIAN JOURNAL OF CHEMISTRY
https://doi.org/10.14233/ajchem.2026.35218

# Studies on the Structural, Optical, Photocatalytic and Luminescence Properties of Monodispersed CdS Nanoparticles Capped with *Moringa oleifera* L. Leaf Extract

B. SRINIVASA GOUD[1,*], Y. SURESH[2], G. ODELU[3], S. ANNAPURNA[4], G. BHIKSHAMAIAH[5] and A.K. SINGH[1,6]

[1]Department of Physics, Vivekananda Govt. Degree College (A), Hyderabad-500044, India
[2]Department of Physics, Osmania University, Hyderabad-500007, India
[3]Department of Botany, Government Degree College, Huzurabad-505468, India
[4]Department of Physics, Veeranari Chakali Ilamma Women's University, Hyderabad-500095, India
[5]Department of Humanities and Sciences, CVR College of Engineering, Ibrahimpatnam (M)-501510, India
[6]Department of Physics and Chemistry, Mahatma Gandhi Institute of Technology, Hyderabad-500075, India

*Corresponding author: E-mail: srinivasgoudbhu@gmail.com

*Received*: 9 November 2025 *Accepted*: 2 January 2026 *Published online*: 6 March 2026 AJC-22284

This study reports the structural, optical, photocatalytic and luminescence properties of monodispersed cadmium sulphide nanoparticles (CdS NPs) synthesised *via* an eco-friendly green synthesis approach using *Moringa oleifera* leaf extract as a natural stabilizing and capping agent. Cadmium nitrate, cadmium sulphate and cadmium chloride are used as cadmium precursors, while sodium sulphide served as the sulphur source. X-ray diffraction (XRD) analysis confirmed the formation of cubic-phase CdS NPs with high crystalline nature. The optical properties are evaluated through UV-Vis absorption spectroscopy, revealing a band gap energy range of 3.08 to 4.92 eV. FTIR confirmed the presence of functional groups responsible for stabilisation of CdS NPs. The morphological characteristics, elemental composition and purity are assessed using FESEM and EDS. Small-angle X-ray scattering (SAXS) and transmission electron microscopy (TEM) determined the nanoparticle size to be below 5 nm, confirming their nanoscale dimensions. Photoluminescence (PL) spectra indicate strong emission properties, enhancing their potential use in optoelectronic applications. The photocatalytic activity of CdS NPs is evaluated by degrading methylene blue (MB) and rhodamine B (RhB) dyes under visible light irradiation, demonstrating their efficiency in environmental remediation and wastewater treatment. The results highlight the superior optical, structural and catalytic performance of *M. oleifera*-capped CdS NPs, making them promising candidates for advanced nanomaterial applications in solar cells, photocatalysis and biomedical fields.

**Keywords: CdS NPs, *Moringa oleifera*, Photocatalysis, Rhodamine B, Methylene blue, Photoluminescence.**

## INTRODUCTION

Nanomaterial synthesis is broadly divided into conventional and green approaches. Conventional methods include chemical precipitation and reduction, co-precipitation, chemical bath deposition, hydrothermal and solvothermal techniques, photochemical processes, ultrasonic irradiation, microwave heating and laser ablation [1-8]. Among these, hydrothermal synthesis enables controlled crystal growth under high temperature and pressure, often employing organic solvents and additives such as thioglycerol, triethanolamine, thiophenol and polymeric stabilizers as templates, capping or passivating agents, though their environmental impact remains a concern.

The second category, green synthesis, adheres to the principles of green chemistry and utilizes microorganisms and plant extracts, which are abundantly available. Nanoparticles (NPs) synthesised *via* traditional methods exhibit advantages such as high scalability [9], controlled morphology and particle size [10], applications in electrical and electronic devices [11], targeted drug delivery [12] and energy storage [13,14]. However, these methods also have significant drawbacks, including the use of toxic organic solvents, high energy consumption and extreme reaction conditions, leading to environmental hazardness [15,16]. Due to these concerns, traditional methods are increasingly being replaced by green synthesis approaches. With rising environmental concerns, researchers are focusing on sustainable green synthesis techniques.

Cadmium sulphide (CdS), a II–VI direct bandgap semiconductor with a bulk bandgap of 2.42 eV at room temperature, crystallizes in orthorhombic, hexagonal and cubic forms.

Its wide bandgap makes CdS suitable for optoelectronic devices including LEDs, photodetectors, photovoltaics, photocatalysts, and heterojunction solar cells [17-23]. Green synthesis of CdS NPs offers eco-friendly advantages such as antimicrobial activity, enhanced stability and biocompatibility. The biomolecules and synthesis parameters govern nanoparticle size and morphology, while plant-derived waste like onion or banana peels can serve as natural capping agents [24-27]. In this study, *Moringa oleifera* leaf extract was employed as a reducing and stabilizing agent, leveraging its phenolic-rich composition. The synthesized CdS NPs were systematically characterized for structural, optical and functional properties, alongside their photocatalytic and photoluminescent performance.

## EXPERIMENTAL

The chemicals and solvents used for the synthesis of cadmium sulphide nanoparticles (CdS NPs) were of analytical grade and used as such. Cadmium chloride monohydrate ($CdCl_2·H_2O$) and L-ascorbic acid ($C_6H_8O_6$) were procured from Central Drug House (P) Ltd., India, while cadmium nitrate tetrahydrate ($Cd(NO_3)_2·4H_2O$) and cadmium sulphate octahydrate ($CdSO_4·8H_2O$) were obtained from FINAR, India. Sodium sulphide hydrate flakes ($Na_2S·H_2O$) were purchased from HiMedia Laboratories Pvt. Ltd., India. Millipore water was used during the synthesis process and deionized water was used for washing to ensure high-purity samples.

**Synthesis of CdS NPs:** CdS NPs were synthesized using a green synthesis approach in which *Moringa oleifera* leaf extract served as a reducing and stabilizing agent, following a modified literature procedure [28]. A 0.1 M $Na_2S·H_2O$ solution was added to the prepared plant extract gradually under vigorous stirring. Separately, 0.1 M cadmium salt solutions were prepared using $CdCl_2·H_2O$ (1.8331 g), $Cd(NO_3)_2·4H_2O$ (2.36 g) and $CdSO_4·8H_2O$ (2.0847 g) in 100 mL Milli-Q water. Each cadmium solution was added slowly to the sulphide extract mixture under continuous stirring, producing a yellow-orange colouration indicating CdS NPs formation. The reaction mixture was maintained at pH 6-11 and stirred at 60 ºC for 4 h to complete nanoparticle formation. The resulting precipitate was washed with methanol, centrifuged and dried to obtain yellow CdS NPs powder.

**Characterisation:** The green synthesized CdS NPs were characterized using multiple analytical techniques. The crystal structure and phase composition were examined by X-ray diffraction (XRD) using a PHILIPS PW1830 generator diffractometer with Cu*K*α radiation (λ = 1.54056 Å) operating at 40 kV and 25 mA. The optical properties were analyzed by UV-Visible spectroscopy (Spectris 2092) over the 190-1100 nm wavelength range. Fourier transform infrared spectroscopy (FTIR) was performed using a Shimadzu FTIR-8400S spectrometer to identify surface functional groups. The surface morphology and particle-size distribution were studied by scanning electron microscopy (SEM) using a ZEISS Special Edition18 instrument, while small-angle X-ray scattering (SAXS) (Xeuss Dual Energy Mo-Cr system, Xenocs, France) was used to determine nanoparticle size distribution. Transmission electron microscopy (TEM) (Philips CM-20, 200 kV) was employed to confirm morphology and average particle size and photoluminescence (PL) spectroscopy (Jobin Yvon Fluorolog-3-11 spectrofluorometer) was used to investigate the emission properties of the CdS NPs.

**Photocatalytic activity:** The photocatalytic activity of the as-prepared CdS NPs was evaluated using methylene blue (MB) and rhodamine B (RhB) as model dyes. For each experiment, 0.05 g of CdS NPs was dispersed in 100 mL aqueous dye solution, ultrasonicated for 10 min and stirred in dark for 1 h to establish adsorption-desorption equilibrium. The suspension was then exposed to solar irradiation under continuous stirring and 2 mL solution was collected at regular intervals for analysis. The degradation of MB and RhB was monitored by recording the decrease in their characteristic absorption peaks using UV-visible spectroscopy, which was used to evaluate the photocatalytic efficiency of the CdS NPs.

## RESULTS AND DISCUSSION

**Structural characterisation:** The structural properties of CdS NPs synthesized using *M. oleifera* leaf extract as a surfactant were examined by XRD technique (Fig. 1a-c). The diffraction peaks observed at 2θ values of 26.55º, 44.01º, 51.62º and 71.46º correspond to the (111), (220), (311) and (420) planes of cubic CdS, respectively [29]. The (111) reflection showed the highest intensity indicating the superior crystal orientation along this plane. A weak additional peak at 2θ values of 32.38º (Fig. 1c) was assigned to the (102) plane of $CdSO_4$ (JCPDS No. 86-1558), suggesting the presence of a minor residual $CdSO_4$ salt. The average crystallite sizes of CdS NPs synthesized using cadmium chloride, cadmium nitrate and cadmium sulphate precursors were estimated to be 3 nm, 2 nm, and 2 nm, respectively. The lattice constant was calculated from the XRD data using eqn. 1:

$$a = d_{hkl} \times \sqrt{(h^2 + k^2 + l^2)} \quad (1)$$

where 'a' represents the lattice constant; 'd' is interplanar spacing; and (*hkl*) are the Miller indices of the crystal planes.

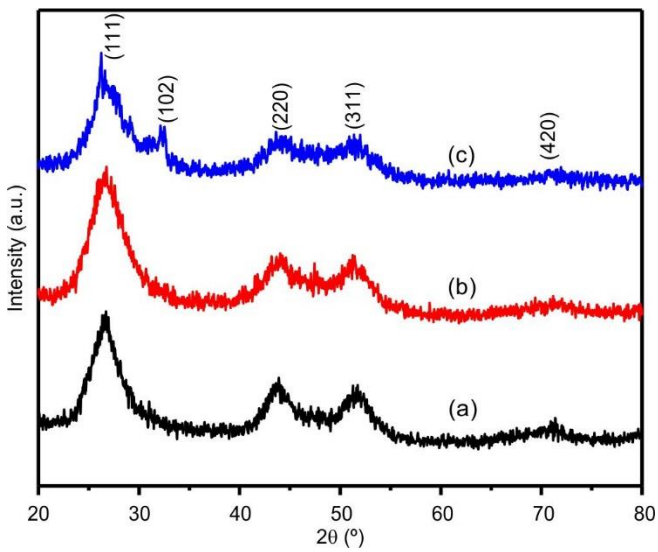


Fig. 1. XRD spectra of *M. oleifera* leaf extract synthesised CdS NPs from different cadmium salts such as (a) cadmium chloride, (b) cadmium nitrate and (c) cadmium sulphate

The calculated lattice constant in this case is 5.8313 Å, which is almost similar to the previously reported value of 5.8304 Å [14].

The diffraction pattern in Fig. 1c indicates the presence of both nanocrystalline and coarse CdS phases, while samples synthesized from cadmium nitrate (Fig. 1b) and cadmium chloride show predominantly nanocrystalline CdS formation.

**Surface morphology:** The SEM images of *M. oleifera* leaf extract mediated CdS NPs synthesized using cadmium chloride, cadmium nitrate and cadmium sulphate are shown in Fig. 2a-c. The SEM micrographs reveal agglomerated CdS NPs with distinct morphologies depending on the precursor salt. The sample prepared using cadmium chloride (Fig. 2a) exhibits a rod-like morphology with inclined orientation, while cadmium nitrate-derived sample (Fig. 2b) shows a flower-like structure formed by dense aggregation of crystallites. The cadmium sulphate-derived sample (Fig. 2c) displays a spherical morphology with visible agglomeration, which is likely due to the cluster growth of nanocrystallites [29].

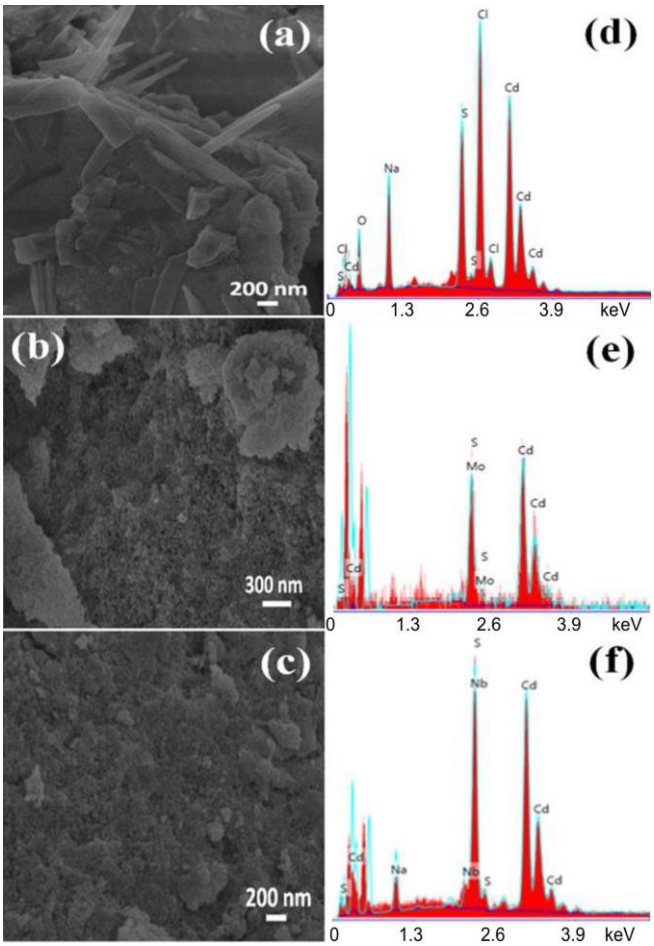


Fig. 2. SEM images (a-c) as well as EDS spectra (d-f) of *M. oleifera* leaves surfactant capped CdS NPs synthesized from (a, d) cadmium chloride, (b, e) cadmium nitrate and (c, f) cadmium sulphate

The corresponding EDS spectra (Fig. 2d-f) confirm the formation of CdS NPs, along with oxygen, sodium and chlorine, indicating the involvement of phytochemical constituents from the *M. oleifera* leaf extract in nanoparticle stabilization [30,31]. The presence of chlorine may also be attributed to residual byproducts formed during the synthesis. The average particle sizes estimated from SEM analysis were 2.56 nm, 3.83 nm and 1.42 nm for CdS NPs synthesized using cadmium chloride, cadmium nitrate and cadmium sulphate, respectively.

Further structural confirmation was obtained from TEM and SAED analysis (Fig. 3a-c). TEM images show well-dispersed nanoscale CdS particles and the particle size distribution histograms indicate average sizes of 2.12 nm, 2.48 nm and 2.73 nm for CdS NPs synthesized from cadmium chloride, cadmium nitrate and cadmium sulphate, respectively. The SAED patterns confirm the cubic crystalline structure of CdS, consistent with XRD and SAXS results.

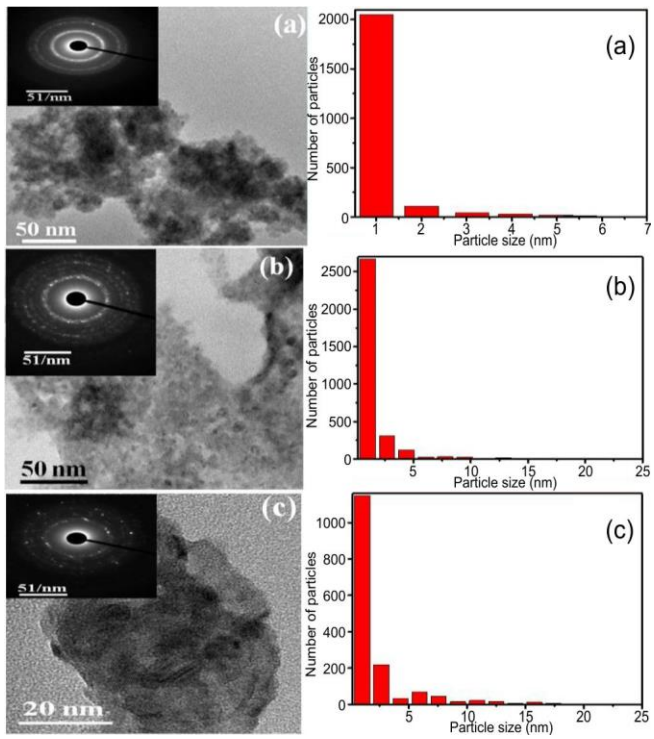


Fig. 3. TEM micrographs and nanoparticle size distribution histograms of *M. oleifera* leaf extract-capped CdS NPs synthesised from different cadmium precursors (a) cadmium chloride, (b) cadmium nitrate and (c) cadmium sulphate

**SAXS studies:** The microstructural characteristics of *M. oleifera* leaf extract mediated CdS NPs were investigated using small-angle X-ray scattering (SAXS). The SAXS intensity profiles and corresponding volume distribution curves for CdS NPs synthesized from cadmium chloride, cadmium nitrate and cadmium sulphate precursors are shown in Fig. 4. The scattering profiles exhibit high intensity in the Porod region ($q > 1$ nm$^{-1}$), with intensity decay consistent with smooth nanoparticle surfaces [32].

SAXS results indicate a narrow particle-size distribution across all samples. The average particle sizes were estimated to be approximately 3.4 nm, 4.8 nm and 4.3 nm for CdS NPs synthesized from cadmium chloride, cadmium nitrate and cadmium sulphate, respectively. These values are in good agreement with XRD and TEM observations, confirming the nanoscale size and relatively uniform dispersion of the CdS NPs [33]. The results also suggest that phytochemical components in *M. oleifera* leaf extract contribute to nanoparticle

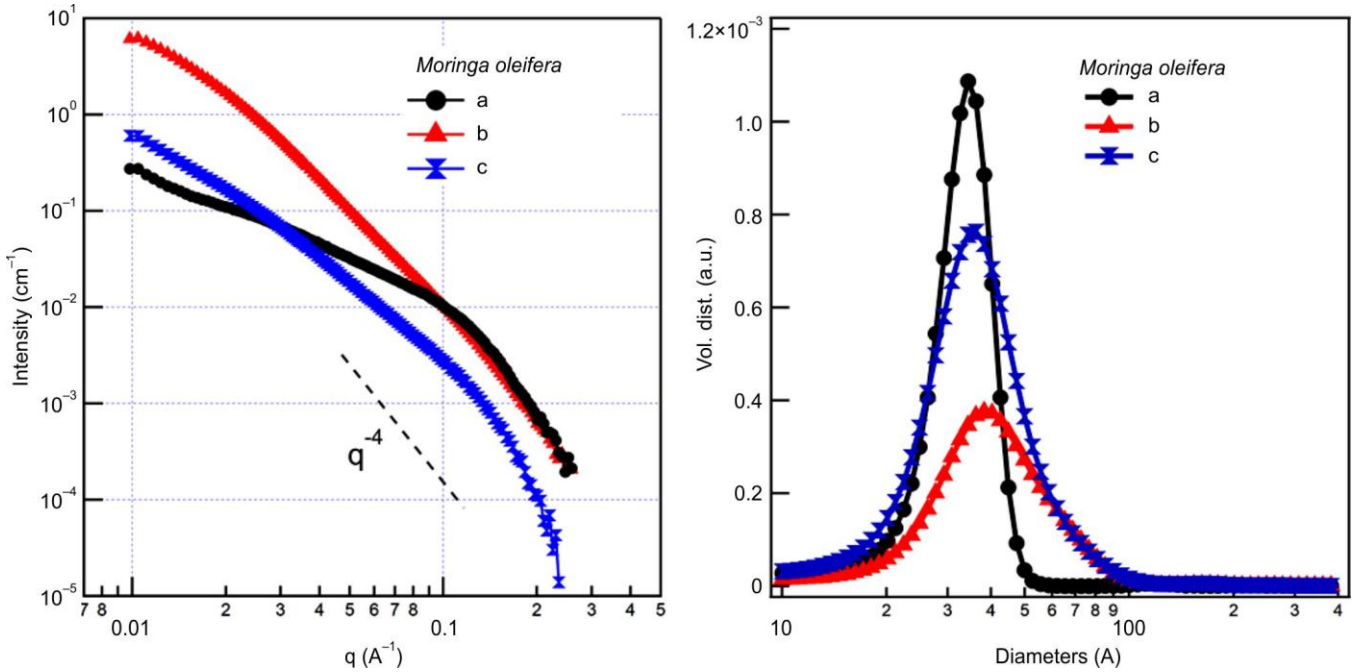


Fig. 4. SAXS patterns and volume distribution curves of *M. oleifera* leaf extract mediated CdS NPs using (a) cadmium chloride, (b) cadmium nitrate and (c) cadmium sulphate

stabilization, promoting controlled nucleation and growth during synthesis [30,31].

**FTIR studies:** Fig. 5a-c show the FTIR spectra of *M. oleifera* leaf extract mediated CdS NPs synthesized using cadmium chloride, cadmium nitrate and cadmium sulphate, while Fig. 5d represents the spectrum of the leaf extract. A broad band around 3451 cm$^{-1}$ is assigned to O–H stretching vibrations, indicating hydroxyl-containing functional groups. The band near 2361 cm$^{-1}$ corresponds to C–H stretching vibrations, while the peak at approximately 1639 cm$^{-1}$ is associated with carbonyl stretching vibrations of protein-related functional groups [34]. Additional peaks observed at 1468, 1382, 1275, 1094 and 595 cm$^{-1}$ correspond to $CH_3/CH_2$ bending in proteins, C–CH bending, C–O stretching and Cd–S stretching vibrations, respectively [35,36]. The presence of these functional groups suggests the involvement of phytochemical constituents from the *M. oleifera* extract in stabilizing the nanoparticles, while the band near 595 cm$^{-1}$ confirms the formation of CdS NPs.

**UV-Visible absorption studies:** Fig. 6a-c show the UV-visible absorption spectra of CdS NPs synthesized using cadmium chloride, cadmium nitrate and cadmium sulphate precursors. The primary absorption peaks observed at approximately 263 nm, 232 nm and 267 nm, respectively, are characteristic of excitonic transitions in semiconductor CdS NPs and indicate the presence of phytochemical stabilizing agents from *M. oleifera* leaf extract [37]. Secondary absorption bands appearing at 451 nm (Fig. 6a), 459 nm (Fig. 6b), and 442 nm (Fig. 6c) are attributed to electronic transitions influenced by particle-size variation, reflecting quantum confinement effects associated with nanoscale CdS particles.

**Band gap energy determination:** The optical band gap energy of CdS NPs was estimated from Tauc plots (Fig. 6d-f) by extrapolating the linear portion of the absorption curve to

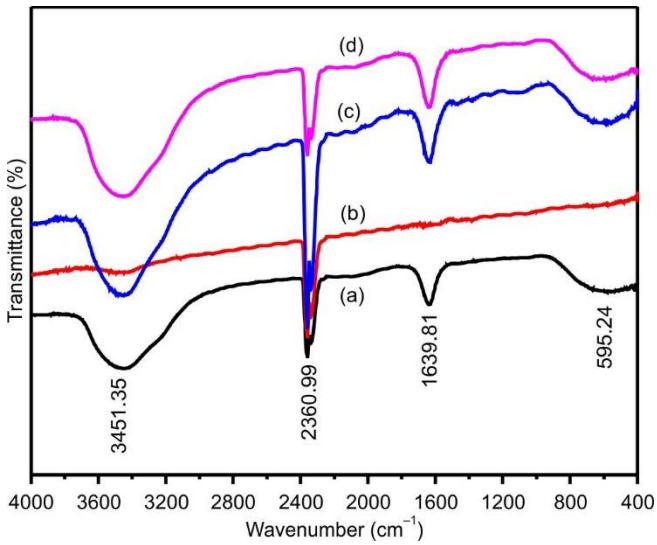


Fig. 5. FTIR spectra of *M. oleifera* leaf extract mediated CdS NPs using different cadmium salts such as (a) cadmium chloride, (b) cadmium nitrate and (c) cadmium sulphate

the energy axis. The calculated band gap values were approximately 4.07-5.08 eV for CdS synthesized from cadmium chloride, 4.70 eV for cadmium nitrate-derived CdS and 3.56 eV for cadmium sulphate-derived CdS. These values are significantly higher than the reported band gap of bulk CdS (2.42 eV) [38], indicating a blue shift in the absorption edge due to quantum confinement effects.

The increased band gap values confirm the size-dependent optical behaviour of nanoscale CdS particles, consistent with the excitonic absorption features observed in Fig. 6a-c. Together, the absorption spectra and Tauc plot analysis demonstrate the influence of particle size and synthesis conditions on the optical properties of CdS NPs.

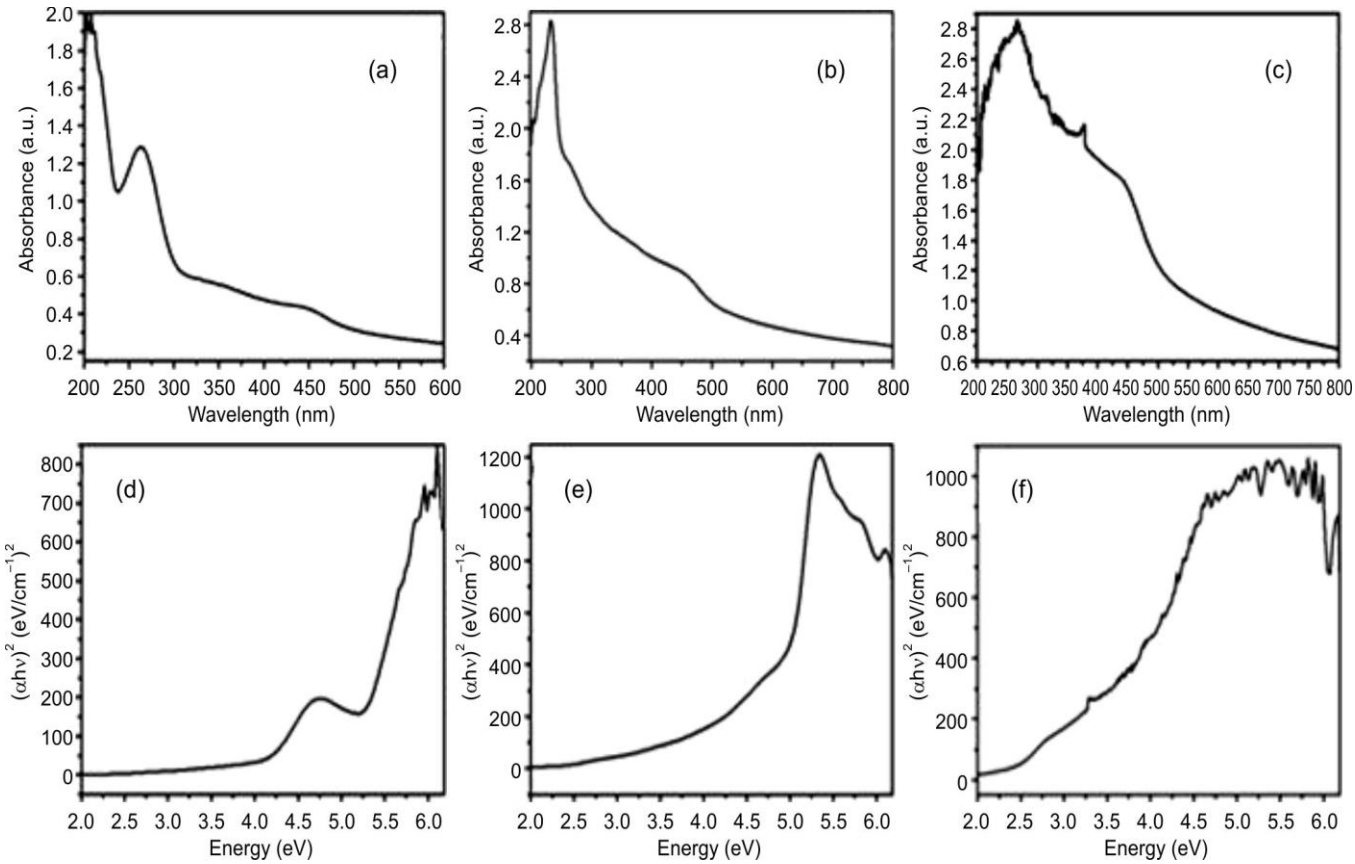


Fig. 6. UV-Vis absorption spectra and Tauc's plot of *M. oleifera* leaf extract-mediated CdS NPs using different cadmium precursors, (a, d) cadmium chloride, (b, e) cadmium nitrate and (c, f) cadmium sulphate

**Catalytic studies:** The photocatalytic performance of *M. oleifera* leaf extract mediated CdS NPs was evaluated through the degradation of methylene blue (MB) and rhodamine B (RhB) under ambient visible-light irradiation for 180 min. The degradation efficiency of MB dye reached 67%, 49% and 43% for CdS NPs synthesized from cadmium chloride, cadmium nitrate and cadmium sulphate precursors, respectively (Fig. 7a-c). The maximum absorption peak in Fig. 7a shifted from 664 nm to 611 nm, corresponding to a blue shift of 53 nm after 120 min (including 60 min in dark and 60 min under visible-light irradiation). This shift indicates photocatalytic degradation of MB and the formation of intermediate decomposition products. Among these, CdS NPs prepared from the cadmium chloride precursor exhibited the highest photocatalytic activity, exhibiting approximately 39% higher degradation efficiency compared with unstabilized CdS NPs, indicating the beneficial role of *M. oleifera* phytochemicals in nanoparticle stabilization and photocatalytic enhancement.

The photocatalytic degradation of RhB dye was monitored by recording the decrease in the characteristic absorption peak at 554 nm over time (Fig. 8a-c). A rapid reduction in dye concentration within 120 min was observed for CdS NPs synthesized using the cadmium chloride precursor, while gradual degradation behaviour was observed for nanoparticles derived from cadmium nitrate and cadmium sulphate precursors. The normalized concentration plot (Fig. 8d) confirms the degradation trend in the presence of the photocatalyst. After 180 min, RhB degradation efficiencies of approximately 45%, 42% and 39% were obtained for CdS NPs synthesised from cadmium chloride, cadmium nitrate and cadmium sulphate precursors, respectively. A minor improvement (3%) in RhB degradation was observed for *M. oleifera* mediated CdS NPs synthesized from the cadmium nitrate precursor compared with unstabilized CdS.

**Photoluminescence (PL) studies:** Fig. 9a-c shows the PL spectra of *M. oleifera* mediated CdS NPs synthesized using cadmium chloride, cadmium nitrate and cadmium sulphate precursors, with excitation at 320 nm. A strong and narrow emission peak at approximately 491 nm (Fig. 9c) is attributed to band-edge luminescence of CdS NPs. In contrast, broader and lower-intensity emission peaks around 514 nm are observed for CdS NPs synthesized from cadmium nitrate and cadmium sulphate, while a weak emission near 509 nm appears for CdS NPs derived from cadmium chloride. These emissions in the 509-514 nm region are associated with defect related luminescence arising from sulphur vacancies, while the variation in emission intensity reflects particle-size dependent quantum confinement effects. The Stokes-shifted luminescence observed in larger CdS clusters can be attributed to mid-bandgap states indicating increased Franck-Condon displacement in the excited state. As nanoparticle size decreases, the bandgap widens and surface defect states become more accessible, leading to enhanced luminescence behaviour [39]. Furthermore, reduced PL intensity near the band-edge region may result from the surface trapping states acting as non-radiative recombination centers [40].

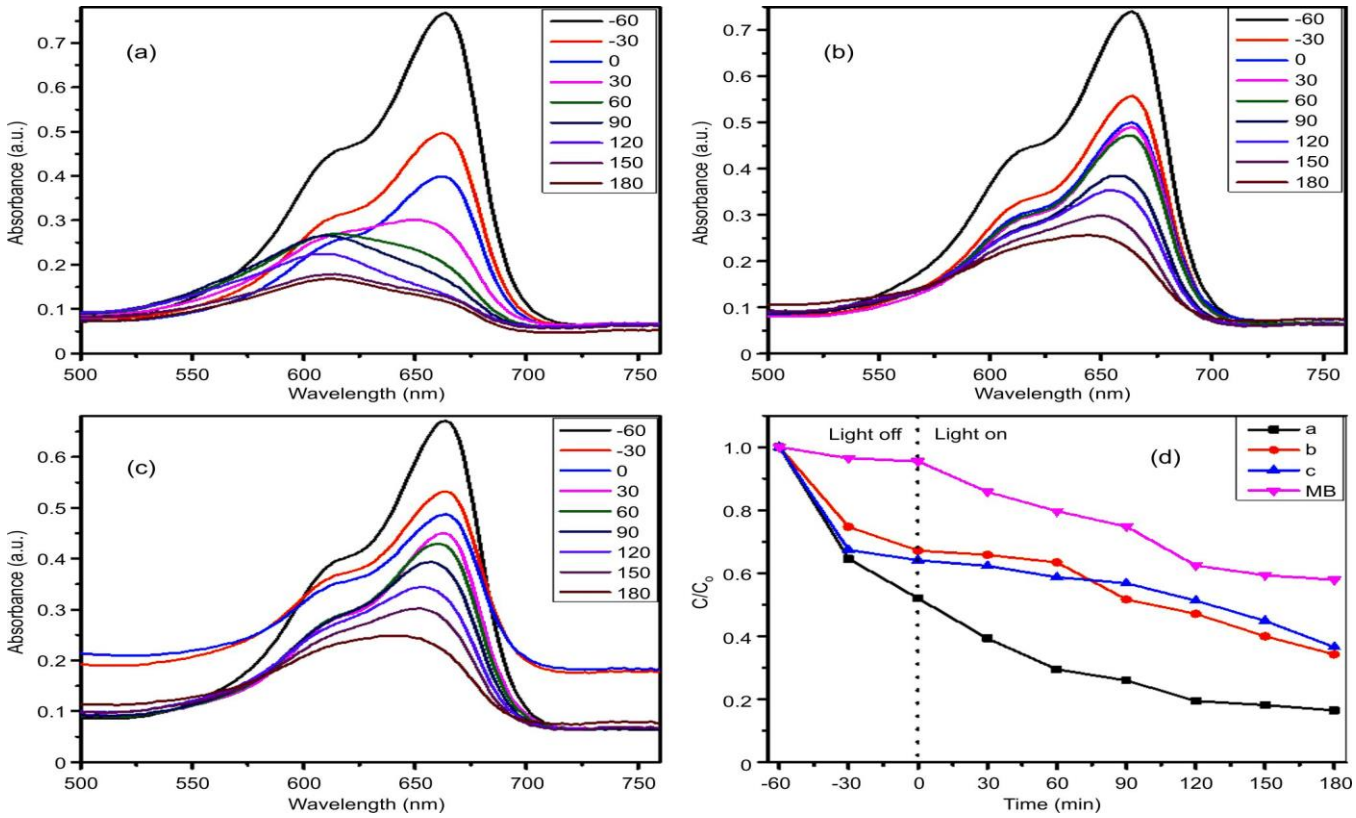


Fig. 7. Photocatalytic degradation of MB using *M. oleifera* leaf extract-mediated CdS NPs using different cadmium precursors, (a) cadmium chloride, (b) cadmium nitrate, (c) cadmium sulphate and (d) reduction in MB absorbance over time

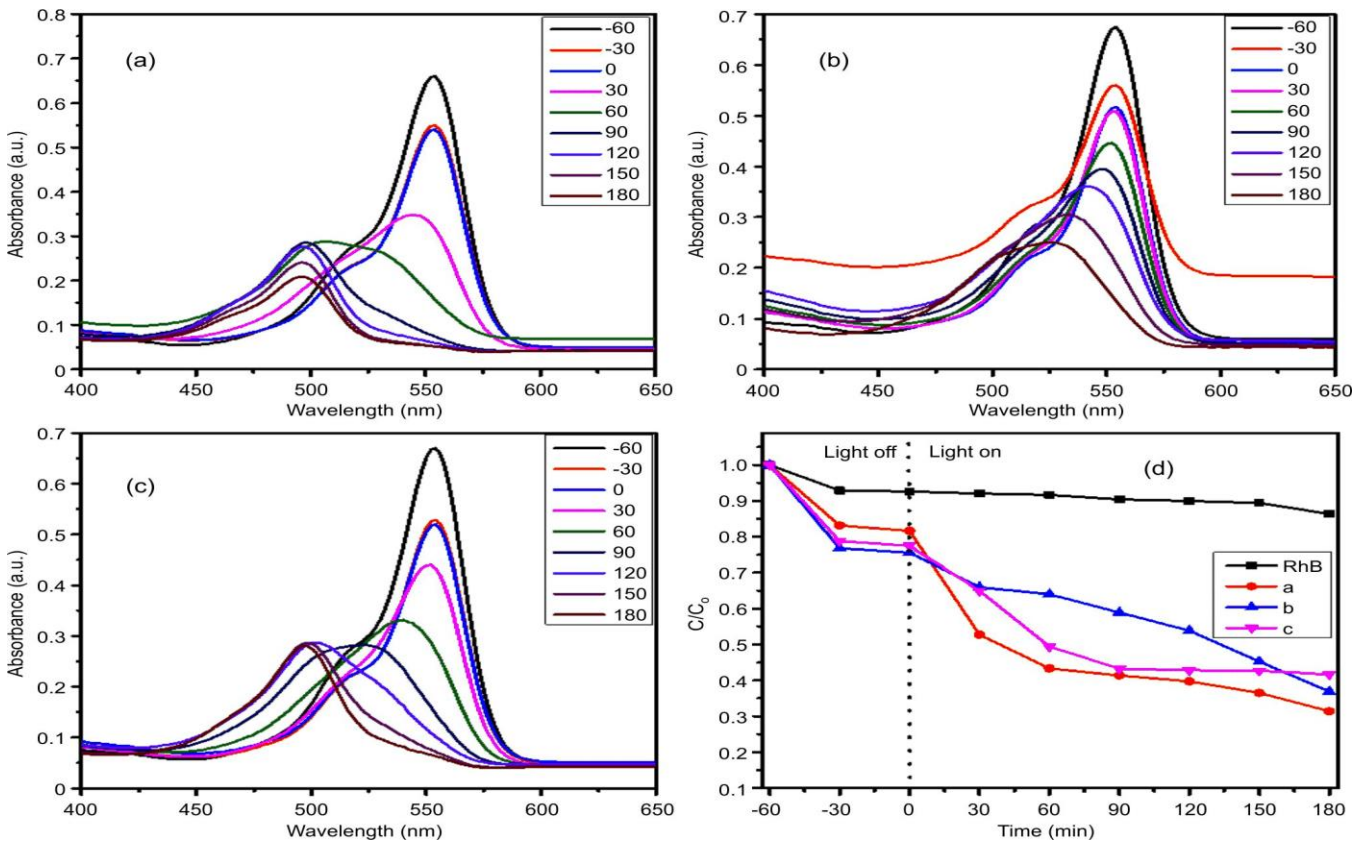


Fig. 8. Photocatalytic degradation of RhB using *M. oleifera* leaf extract-mediated CdS NPs using different cadmium precursors, (a) cadmium chloride, (b) cadmium nitrate, (c) cadmium sulphate and (d) reduction in RhB absorbance over time

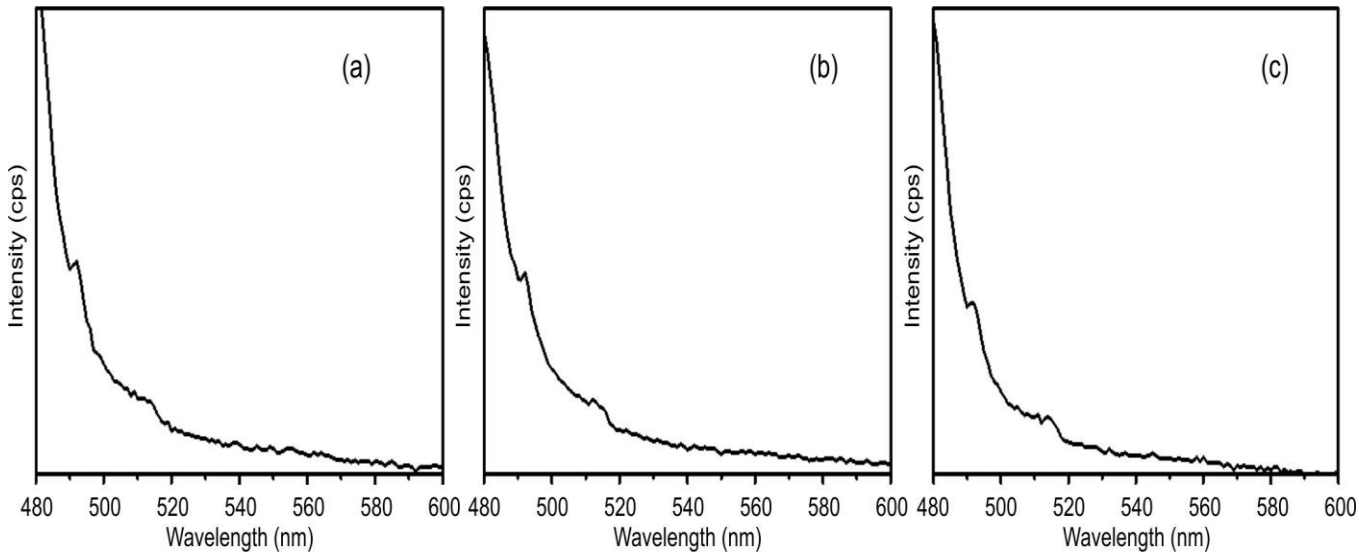


Fig. 9. Photoluminescence emission spectra of *M. oleifera* leaf extract-mediated CdS NPs using different cadmium precursors, (a) cadmium chloride, (b) cadmium nitrate, and (c) cadmium sulphate

## Conclusion

Green-synthesised CdS NPs were successfully synthesised using *Moringa oleifera* leaf extract as a natural stabilizing agent. Cadmium nitrate, cadmium sulphate and cadmium chloride were utilised as cadmium precursors, while sodium sulphide served as sulphur source. The structural analyses confirmed the formation of uniform nanoscale CdS particles (3-5 nm) with reduced agglomeration. Optical studies showed size-dependent band gap values (3.56-5.08 eV), indicating quantum confinement effects. All the CdS NPs samples exhibited dominant band-edge photoluminescence emission, suggesting low defect density and good structural quality. The synthesized CdS NPs also demonstrated effective photocatalytic degradation of methylene blue (67%) and rhodamine B (45%) under visible light, with the cadmium chloride derived sample showing the highest activity. Thus, the green synthesis approach provides a simple and environmentally friendly route to CdS NPs with promising photocatalytic and optoelectronic potential.

## ACKNOWLEDGEMENTS

The authors would like to express their sincere gratitude to the Head of Department, Department of Physics, Osmania University, Hyderabad, for their valuable support. The authors also extend their heartfelt thanks to the Director, Defence Metallurgical Research Laboratory (DMRL), Hyderabad, for providing necessary resources and assistance. Furthermore, the authors whole heartedly acknowledge the Sophisticated Analytical Instrument Facility (SAIF), IIT Chennai, for granting access to experimental facilities essential for this study.

## CONFLICT OF INTEREST

The authors declare that there is no conflict of interests regarding the publication of this article.

## DECLARATION OF AI-ASSISTED TECHNOLOGIES

During the preparation of this manuscript, the authors used an AI-assisted tool(s) to improve the language. The authors reviewed and edited the content and take full responsibility for the published work.

## REFERENCES

1. Z.L. Wang, *Mater. Today*, **7**, 26 (2004); https://doi.org/10.1016/S1369-7021(04)00286-X
2. L.V. Srinivasan and S.S. Rana, *Discov. Appl. Sci.*, **6**, 371 (2024); https://doi.org/10.1007/s42452-024-06040-8
3. S. Kumari, S. Raturi, S. Kulshrestha, K. Chauhan, S. Dhingra, A. Kovács, K. Thu, R. Khargotra and T. Singh, *J. Mater. Res. Technol.*, **27**, 1739 (2023); https://doi.org/10.1016/j.jmrt.2023.09.291
4. S.H. Tadesse and T.T. Hailemariam, *Advances*, **6**, 63 (2025); https://doi.org/10.11648/j.advances.20250602.15
5. N. Baig, I. Kammakakam, and W. Falath, *Mater. Adv.*, **2**, 1821 (2021); https://doi.org/10.1039/D0MA00807A
6. P. Szczyglewska, A. Feliczak-Guzik, and I. Nowak, *Molecules*, **28**, 4932 (2023); https://doi.org/10.3390/molecules28134932
7. M.A.B. Turki and T.A. Salman, *J. Chem. Rev.*, **6**, 458 (2024); https://doi.org/10.48309/jcr.2024.468135.1350
8. N.H. Nam and N.H. Luong, in eds.: V. Grumezescu and A.M. Grumezescu, Nanoparticles: Synthesis and Applications, In: Materials for Biomedical Engineering, Inorganic Micro and Nanostructures, Elsevier, Chap. 7, pp. 211-240 (2019).
9. A. Vinukonda, N. Bolledla, R.K. Jadi, R. Chinthala and V. R. Devadasu, *Next Nanotechnol.*, **8**, 100169 (2025); https://doi.org/10.1016/j.nxnano.2025.100169
10. V. Harish, M.M. Ansari, D. Tewari, M. Gaur, M.-L. García-Betancourt, A.B. Yadav, F.M. Abdel-Haleem, M. Bechelany and A. Barhoum, *Nanomaterials*, **12**, 3226 (2022); https://doi.org/10.3390/nano12183226
11. I. Matsui, *J. Chem. Eng. Japan*, **38**, 535 (2005); https://doi.org/10.1252/jcej.38.535
12. J. Panyam, M.M. Dali, S.K. Sahoo, W. Ma, S.S. Chakravarthi, G.L. Amidon, R.J. Levy and V. Labhasetwar, *J. Control. Release*, **92**, 173 (2003); https://doi.org/10.1016/S0168-3659(03)00328-6

13. P.G. Bruce, B. Scrosati and J.M. Tarascon, *Angew. Chem. Int. Ed.*, **47**, 2930 (2008); https://doi.org/10.1002/anie.200702505
14. A.S. Arico, P. Bruce, B. Scrosati, J.M. Tarascon and W. van Schalkwijk, *Nat. Mater.*, **4**, 366 (2005); https://doi.org/10.1038/nmat1368
15. B.L. Cushing, V.L. Kolesnichenko and C.J. O'Connor, *Chem. Rev.*, **104**, 3893 (2004); https://doi.org/10.1021/cr030027b
16. S.M. Gupta and M. Tripathi, *Mater. Sci. Technol.*, **27**, 1 (2011); https://doi.org/10.1179/026708310X12815992418418.
17. K.A. Altammar, *Front. Microbiol.*, **14**, 1155622 (2023); https://doi.org/10.3389/fmicb.2023.1155622
18. A.S.Z. Lahewil, Y. Al-Douri, U. Hashim and N.M. Ahmed, *Solar Energy*, **86**, 3234 (2012); https://doi.org/10.1016/j.solener.2012.08.013
19. N.V. Hullavarad, S.S. Hullavarad and P.C. Karulkar, *J. Nanosci. Nanotechnol.*, **8**, 3272 (2008); https://doi.org/10.1166/jnn.2008.145
20. L.A. Carrasco-Chavez, J.F. Rubio-Valle, A. Jiménez-Pérez, J.E. Martín-Alfonso and A. Carrillo-Castillo, *Micromachines*, **14**, 1168 (2023); https://doi.org/10.3390/mi14061168
21. M. Rajesh and K. Ramamoorthy, *J. Nanopart. Res.*, **21**, 82 (2019); https://doi.org/10.1007/s11051-019-4525-2
22. R. Singh and P. Kumar, *Mater. Today Proc.*, **29**, 491 (2020); https://doi.org/10.1016/j.matpr.2019.12.149
23. J.P. Enríquez and X. Mathew, *Sol. Energy Mater. Sol. Cells*, **76**, 313 (2003); https://doi.org/10.1016/S0927-0248(02)00283-0
24. M. Khan, M.R. Shaik and S.F. Adil, *Environ. Nanotechnol. Monit. Manag.*, **8**, 99 (2017); https://doi.org/10.1016/j.enmm.2017.06.004
25. P. Rattanakit, K. Wongyai, B. Ngamsom and P. Saensuk, *Green Technol. Sustain.*, **4**, 100284 (2026); https://doi.org/10.1016/j.grets.2025.100284
26. M.F. Baran, C. Keskin, A. Hatipoğlu, M. Yildiztekin, S. Küçükaydin, A. Baran, K. Kurt, H. Hoşgören, M.M.R. Sarker, A. Sufianov, O. Beylerli, R. Khalilov and A. Eftekhari, *Molecules*, **28**, 2310 (2023); https://doi.org/10.3390/molecules28052310
27. A. Bankar, B. Joshi, A. R. Kumar, and S. Zinjarde, Colloids Surf. B Biointerfaces, **80**, 45 (2010); https://doi.org/10.1016/j.colsurfb.2010.05.029
28. M.A. Kandeil, E.T. Mohammed, K.S. Hashem, L. Aleya and M.M. Abdel-Daim, *Environ. Sci. Pollut. Res. Int.*, **27**, 19169 (2020); https://doi.org/10.1007/s11356-019-05514-2
29. B.R. Sankapal, R.S. Mane and C.D. Lokhande, *Mater. Res. Bull.*, **35**, 177 (2000); https://doi.org/10.1016/S0025-5408(00)00210-5
30. S. Naranthatta, P. Janardhanan, R. Pilankatta and S.S. Nair, *ACS Omega*, **6**, 8646 (2021); https://doi.org/10.1021/acsomega.1c00519
31. M.S. Kiran, C.R. Rajith Kumar, U.R. Shwetha, H.S. Onkarappa, V.S. Betageri and M.S. Latha, *Chem. Data Collect.*, **33**, 100714 (2021); https://doi.org/10.1016/j.cdc.2021.100714
32. T. Li, A.J. Senesi and B. Lee, *Chem. Rev.*, **116**, 11128 (2016); https://doi.org/10.1021/acs.chemrev.5b00690
33. A.K. Keshari and A.C. Pandey, *J. Nanosci. Nanotechnol.*, **8**, 1221 (2008); https://doi.org/10.1166/jnn.2008.370
34. A. Aghajanyan, M. Timotina, T. Manutsyan, A. Harutyunyan, R. Schubert, M. Ginovyan, S. Aydinyan, K. Trchounian, L. Gabrielyan and L. Gabrielyan, *Sci. Rep.*, **15**, 16637 (2025); https://doi.org/10.1038/s41598-025-01023-0
35. S.R.K. Pandian, V. Deepak, K. Kalishwaralal and S. Gurunathan, *Enzym. Microb. Technol.*, **48**, 319 (2011); https://doi.org/10.1016/j.enzmictec.2011.01.005
36. A. Ullah, S. Rasheed, I. Ali and N. Ullah, *Chem. Rev. Lett.*, **4**, 98 (2021); https://doi.org/10.22034/CRL.2021.262754.1097
37. R.R. Prabhu and M.A. Khadar, *Pramana – J. Phys.*, **65**, 801 (2005); https://doi.org/10.1007/BF02704078.
38. S.K. Azad, M.P. Shah, M.K. Gangwar, P.D. Kunjadia, M. Kumari, F. Ameen and K.S. Prasad, *J. Water Process Eng.*, **82**, 109534 (2026); https://doi.org/10.1016/j.jwpe.2026.109534
39. V. Nogriya, J.K. Dongre, M. Ramrakhiani and B.P. Chandra, *Chalcogenide Lett.*, **5**, 365 (2008).
40. L. Saravanan, S. Diwakar, R. Mohankumar, A. Pandurangan and R. Jayavel, Nanomater. Nanotechnol., **1**, 42 (2011); https://doi.org/10.5772/50959